Supporting Information

Mechanism of nucleated conformational conversion of Aβ42

Ziao Fu[1], Darryl Aucoin[1], Judianne Davis[2], William E. Van Nostrand[2] and Steven O. Smith[1]*

[1]Department of Biochemistry and Cell Biology, Stony Brook University, Stony Brook, NY 11794-5215

[2]Departments of Neurosurgery and Medicine, Stony Brook University, Stony Brook, NY 11794-8122

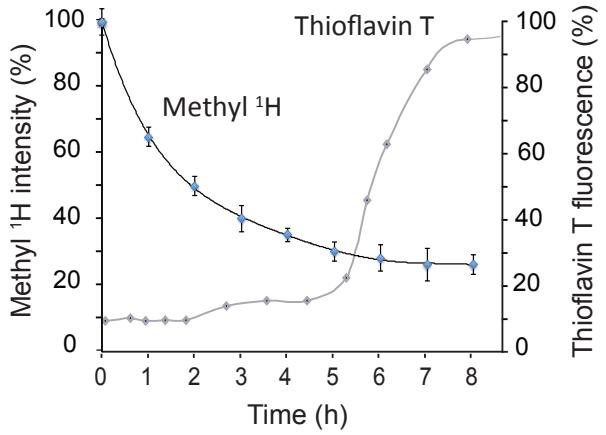

Supplementary Figure 1: Methyl ^{1}H NMR intensity as a function of time. Intensity of methyl resonances from 1D ^{1}H NMR spectra of Aβ42 as a function of incubation time starting with 200 μM monomeric Aβ42. The NMR intensity is plotted on the same time scale as thioflavin T fluorescence intensity measured from a starting solution of 200 μM monomeric Aβ42.

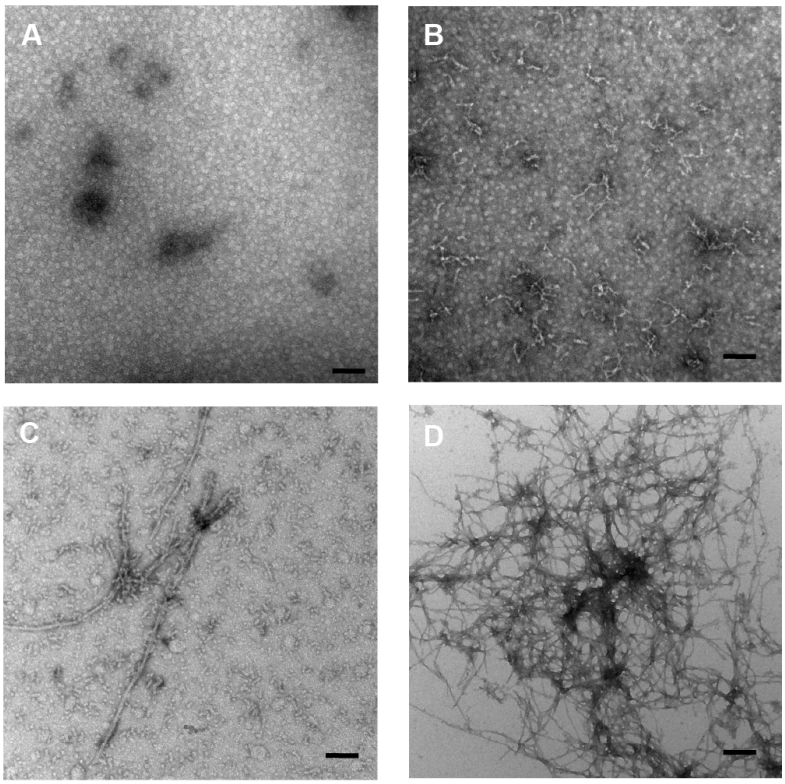

Supplementary Figure 2: Transmission electron microscopy of Aβ42 oligomers, protofibrils and fibrils. To further track the changes in the state of Aβ42 aggregation during incubation at 37 °C, TEM images were obtained of Aβ42 after 0 h (**A**), 6 h (**B**), 8 h (**C**), and 12 days (**D**) at a concentration of 200 μM. The scale bar corresponds to ~100 nm in panels (**A-C)** and ~250 nm in panel (**D)**.

The TEM images provide only a qualitative view of the aggregation pathway. During the time course between 0 and 8 hours, the sample converts from a solution composed of oligomers to one of oligomers and protofibrils. After 8 hours, Aβ42 fibrils appear, although there are typically still a large number of protofibrils. The protofibrils are wavy, elongated structures with lengths of up to ~100 nm. Fibrils are straight structures with lengths over 1 μm. It typically takes several days for the Aβ42 to convert to mature fibrils (with no detectable protofibrils).

The TEM images were obtained using an FEI Tecnai 12 BioTwin 80 kV transmission electron microscope. The sample was diluted to a concentration of 15 μM, deposited onto carbon-coated copper mesh grid and negatively stained for one minute with a 0.5-2% (w/v) uranyl acetate solution. The remaining solution was wicked off using filter paper. The sample was allowed to air dry and digital images were taken with an Advanced Microscopy Techniques camera. Similar results were obtained with Quantifoil Holey carbon grids (1.2/1.3) with a thin carbon film that had been glow-discharged to make the surface hydrophilic.

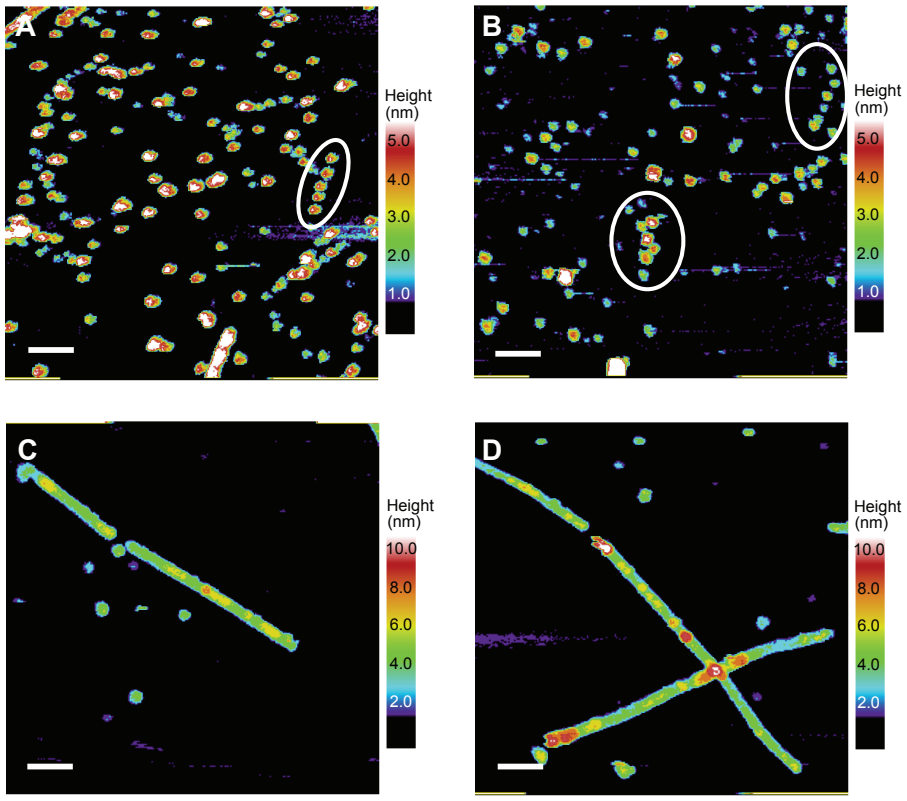

Supplementary Figure 3: AFM of Aβ42 oligomers, protofibrils and fibrils. Additional images are shown of oligomers and protofibrils (panels **A** and **B**) and fibrils (**C** and **D**) obtained by single touch AFM after 6 h and 8 h of incubation at 37 °C, respectively. The images in panel (**A)** show mostly high MW oligomers, many of which have laterally associated into protofibrils (white ellipses). In contrast, the images in panel (**B**) show a mixture of low and high MW oligomers. As in the **Figure 4** (main text), the oligomers that have laterally associated can be composed of both low and high MW oligomers. While many of the images of laterally associated oligomers appear linear, there are also laterally associated oligomers that are non-linear and similar to the curvilinear protofibrils typically observed by TEM.

The gaps between oligomers within a protofibril are attributed to several factors. First, the oligomers are loosely associated at early times in the aggregation process as suggested by the ability to reverse aggregation by dilution. These gaps are lost as the oligomers merge and the protofibrils convert into fibrils. Second, the compressive force applied to the protofibril allows the AFM probe to contact the mica surface in these regions of weakly associated protein. Repeated scanning can disrupt the oligomer association (see *Supporting Figure 4*). The compressive forces with our single touch, low force AFM are on the order of 30-100 pN. While this is 1-2 orders of magnitude lower than typical tapping mode AFM (which also requires multiple contacts with the sample per pixel), it likely results in some sample distortion. Finally,

we cannot rule out that association of the loosely associated oligomers with the mica surface disrupts their interaction.

The low MW oligomers appear to have two distinct surfaces, where one surface is able to mediate the association to form the high MW species. This face-to-face interaction explains the lack of 18-mers observed in our AFM studies as well as in the previous mass spectrometry experiments [1]. One can speculate that the interacting surface is more hydrophobic. We find that the oligomers associate strongly with the polar mica surface in AFM. In AFM studies using graphite that has a hydrophobic surface, more fibril-like structures are observed, suggesting that the hydrophobic surface destabilizes the oligomers and serves as template for fibril formation [2].

These samples were incubated at 200 μM and diluted to 0.5 μM for imaging. The white scale bars for lateral distances are 40 nm. Note that the colored height scales to the right of each figure have a maximum of 5.0 nm in panels (**A**) and (**B**), and 10.4 nm in panels (**C)** and (**D)**.

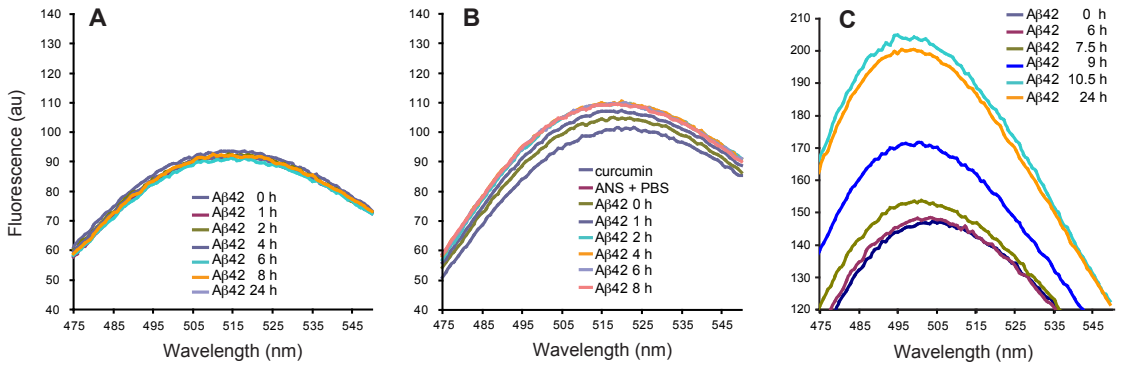

Supplementary Figure 4: ANS fluorescence of Aβ42. ANS (1-anilinonaphthalene-8-sulfonate) undergoes a change in fluorescence upon binding to hydrophobic surfaces,[3,4] and has been used to characterize the surfaces of Aβ oligomers and fibrils.[5-8] To measure the rates of formation and decay of oligomers that are intermediates in the pathway to fibril formation, we studied changes in ANS fluorescence as a function of incubation time over a range of different temperature and salt concentrations. In panel (**A**), we show that there is no change in ANS fluorescence with Aβ42 at 4 °C over 24 hours.

In panel (**B**), we show that curcumin at a 1:1 molar ratio with Aβ42 blocks the increase in ANS fluorescence. We have recently shown that curcumin binds to the N-terminus (residues 5-20) of Aβ42 monomers and cap the height of the oligomers that are formed at 1-2 nm. [9]

In panel (**C**), Bis-ANS, a derivative of ANS, has been used to characterize oligomer formation, and was recently found to be an inhibitor of Aβ42 fibrillization with greater affinity for Aβ42 than ANS.[7] We present the fluorescence spectra of Bis-ANS for comparison with the measurements using ANS. Fluorescence spectra obtained over 24 h are shown of Bis-ANS with Aβ42 at 37 °C in low salt. In a similar fashion to ANS, there is an increase in fluorescence intensity after 6 h of incubation. However, unlike ANS the fluorescence levels do not decrease after 8 h. This difference may reflect a stronger affinity of Bis-ANS for protofibrils and fibrils.

References – Supporting Information

(1) Bernstein, S. L., Dupuis, N. F., Lazo, N. D., Wyttenbach, T., Condron, M. M., Bitan, G., Teplow, D. B., Shea, J., Ruotolo, B. T., Robinson, C. V., and Bowers, M. T. (2009) Amyloid-β protein oligomerization and the importance of tetramers and dodecamers in the aetiology of Alzheimer's disease. *Nat. Chem. 1*, 326-331.

(2) Kowalewski, T., and Holtzman, D. M. (1999) In situ atomic force microscopy study of Alzheimer's β-amyloid peptide on different substrates: new insights into mechanism of β-sheet formation. *Proc. Natl. Acad. Sci. USA 96*, 3688-3693.

(3) Hawe, A., Sutter, M., and Jiskoot, W. (2008) Extrinsic fluorescent dyes as tools for protein characterization. *Pharmaceutical Research 25*, 1487-1499.

(4) Matthews, C. R. (1993) Pathways of protein-folding. *Annu. Rev. Biochem. 62*, 653-683.

(5) Bolognesi, B., Kumita, J. R., Barros, T. P., Esbjorner, E. K., Luheshi, L. M., Crowther, D. C., Wilson, M. R., Dobson, C. M., Favrin, G., and Yerbury, J. J. (2010) ANS binding reveals common features of cytotoxic amyloid species. *ACS chemical biology 5*, 735–740.

(6) Chen, Y. R., and Glabe, C. G. (2006) Distinct early folding and aggregation properties of Alzheimer amyloid-β peptides Aβ40 and Aβ42 - Stable trimer or tetramer formation by Aβ42. *J. Biol. Chem. 281*, 24414-24422.

(7) Ferrao-Gonzales, A. D., Robbs, B. K., Moreau, V. H., Ferreira, A., Juliano, L., Valente, A. P., Almeida, F. C. L., Silva, J. L., and Foguel, D. (2005) Controlling beta-amyloid oligomerization by the use of naphthalene sulfonates - Trapping low molecular weight oligomeric species. *J. Biol. Chem. 280*, 34747-34754.

(8) Ji, S. R., Wu, Y., and Sui, S. F. (2002) Study of the correlation of secondary structure of beta-amyloid peptide (A beta 40) with the hydrophobic exposure under different conditions. *General Physiology and Biophysics 21*, 415-427.

(9) Fu, Z., Aucoin, D., Ahmed, M., Ziliox, M., Van Nostrand, W. E., and Smith, S. O. (2014) Capping of A beta 42 Oligomers by Small Molecule Inhibitors. *Biochemistry 53*, 7893-7903.